remote sensing

MDPI

Article

Assessment of Errors Caused by Forest Vegetation Structure in Airborne LiDAR-Derived DTMs

Jake E. Simpson [1,*], Thomas E. L. Smith [1] and Martin J. Wooster [1,2]

[1] King's College London, Department of Geography, London WC2R 2LS, UK; thomas.smith@kcl.ac.uk (T.E.L.S.); martin.wooster@kcl.ac.uk (M.J.W.)

[2] NERC National Centre for Earth Observation (NCEO), King's College London, London WC2R 2LS, UK

* Correspondence: jake.simpson@kcl.ac.uk

Received: 22 September 2017; Accepted: 26 October 2017; Published: 28 October 2017

Abstract: Airborne Light Detection and Ranging (LiDAR) is a survey tool with many applications in forestry and forest research. It can capture the 3D structure of vegetation and topography quickly and accurately over thousands of hectares of forest. However, very few studies have assessed how accurately LiDAR can measure surface topography under forest canopies, which may be important, for example, in relation to analysis of pre- and post-burn surface height maps used to quantify the combustion of organic soils. Here, we use ground survey equipment to assess digital terrain model (DTM) accuracy in a deciduous broadleaf forest, during both leaf-on and leaf-off conditions. Using the leaf-on LiDAR dataset we quantitatively assess vertical vegetation structure, and use this as a categorical explanatory variable for DTM accuracy. In the presence of leaf-on vegetation, DTM accuracy is severely reduced, with low-stature undergrowth vegetation (such as ferns) causing the greatest errors (RMSE > 1 m). Errors are lower under leaf-off conditions (RMSE = 0.22 m), but still of a magnitude similar to that reported for mean depths of burn in fires involving organic soils. We highlight the need for adequate ground control schemes to accompany any forest-based airborne LiDAR survey which require highly accurate DTMs.

Keywords: airborne LiDAR; DTM; accuracy assessment; vertical vegetation structure; ground control points

1. Introduction

Airborne Laser Scanning (ALS) is a technology used to map the three-dimensional structure of the terrestrial environment for diverse applications such as construction, archaeology, flood modelling and forest science. The method employs a Light Detection and Ranging (LiDAR) scanner mounted aboard an aircraft, which times the return of emitted laser pulses from surfaces on or near the ground, measuring the distance to the object from the sensor. In a forest environment, ALS data can be used to extract useful information for researchers and foresters; e.g., Digital Terrain Models (DTMs) are models of the ground surface, Canopy Height Models (CHMs) are reconstructions of the upper limits of the forest canopy, and vertical and horizontal structural characteristics such as number of strata [1] and crown dimensions [2,3] are useful for allometric estimations of above ground biomass (AGB) of forests. DTMs are perhaps the most important LiDAR-derived forest metric, because the accuracy of nearly all other models and metrics are dependent on them. Examples of typical DTM accuracies achieved for each biome are given in Table 1, showing there are very few DTM accuracy reports in temperate deciduous forest environments.

Table 1. Vertical accuracies reported in previous studies along with their respective biomes and references. The vertical accuracy metric differs between studies, therefore their reporting method is defined in the "Metric" column.

Source	Biome	Vertical Accuracy (m)	Metric
[4]	Old growth tropical forest	1.95	RMSE
[4]	Secondary tropical forest	1.44	RMSE
[4]	Selectively logged tropical forest	1.62	RMSE
[5]	Steep Mediterranean shrubland	0.13–0.41	RMSE
[6]	Temperate conifer	0.21	RMSE
[7]	Temperate conifer	−0.05/0.12	Mean/SD
[8]	Temperate conifer	0.31/0.29	Mean/SD
[9]	Temperate conifer	0.59	RMSE
[10]	Temperate conifer	0.24	RMSE
[11]	Temperate deciduous and conifer	1.22	RMSE
[11]	Temperate grass	0.37	RMSE
[12]	Temperate mixed	0.38	N/A
[11]	Temperate pine	0.45	RMSE
[11]	Temperate shrub	1.53	RMSE
[13]	Tropical forest	1.8	Mean
[14]	Tropical forest	0.43	RMSE
[15]	Tropical forest	0.37	RMSE
[4]	Tropical swamp forest	1.64	RMSE
[16]	Tropical swamp forest	0.16 and 0.41	RMSE
[17]	Tropical swamp forest	0.12	RMSE
[17]	Tropical swamp forest burn scar	0.19	RMSE

DTM accuracy can be affected by horizontal and vertical accuracy of survey instruments (e.g., Global Navigation Satellite Systems (GNSS), total stations (TS), inertial measurement units (IMU) aboard aircraft [18], data collection parameters, site characteristics, data processing methods and algorithms. Typically, the highest quality GNSS equipment can give point coordinates accurate to better than 1 cm in open-sky conditions (i.e., no canopy cover, which may block satellite signals [19]), whereas total station measurements are not affected by canopy cover, and point accuracy can be 2–3 mm. ALS point cloud vertical accuracy is usually reported at approximately 1–20 cm [5,17,20–23]. Data collection parameters include instrument parameters such as mirror tilt angle [24], laser pulse density and flight height [7], and scan angle [25]. Influential site characteristics include the presence of vegetation and/or slope, which are the largest contributors to DTM error, causing errors exceeding those caused by instrumental or methodological error [4,5,7,8,15,22]. Furthermore, point cloud classification algorithms may also induce DTM errors by misclassifying understory or ground-cover vegetation as ground returns, this might be particularly problematic in open-canopy forest where undergrowth may be particularly dense [17,26].

DTM accuracy assessments are a major challenge in forest environments because of the need to measure the position of "true" ground control points, which are independent of the influences of vegetation. It is difficult to take GNSS control points under leaf-on canopies because the satellite signals are blocked by the water in the canopy leaves, and undergrowth density can block the line of sight between the total station instrument and the survey prisms [15,27]. Perhaps for these reasons, very few studies have formally assessed how vertical vegetation structure can affect DTM accuracy in broadleaf forests (Table 1). In leaf-off conditions, such as in winter in deciduous forests, or after a major forest fire, the canopy may open sufficiently to take the type of accurate ground control points required to assess DTM accuracy [11,28].

To date no studies have applied a generic vertical vegetation structure metric as an explanatory variable of DTM accuracy, and most studies reporting DTM accuracy have not quantitatively assessed overlying vegetation structure [7,8,17,20,22]. In situations where it is important to produce highly accurate DTMs (especially in places where ground control points cannot be collected reliably,

e.g., in dense forests), there is a need to identify areas which may be prone to larger errors, so that uncertainty can be quantified adequately.

Vertical vegetation structure can be measured using ALS point cloud data and applied across different forest types [1,29,30]. Gap probability (Pgap) can be calculated from discrete return LiDAR data, and is the proportion of vegetation returns reflected at a given height to the number of returns per plot (including the number of ground returns). Pgap reflects how much vegetation is obstructing the ground at a given height, and can therefore be applied to any classified ALS point cloud to compare different forest environments. It serves as a much more descriptive metric than (e.g.,) canopy height, which provides no information about the vegetation structure between the ground and the top of the canopy [1].

The aim of this study is to assess how vertical vegetation structure affects DTM accuracy in a heterogenous forest plot. The objectives are:

1. Using a network of ground control points (from a GNSS and TS) to produce a reference DTM to assess the accuracy of ALS-derived DTMs.
2. Compare the accuracy of DTMs from ALS surveys in both leaf-on and leaf-off conditions.
3. Quantitatively classify the different vertical vegetation structure categories in the forest plot, and compare DTM accuracy in each category.
4. Compare DTM accuracy with vegetation density at different vertical strata, independently of vertical vegetation structure categories.

2. Site Description, Materials and Methods

Wytham woods is a 400 ha mixed deciduous ancient and secondary woodland situated northeast of Oxford, Oxfordshire, UK (51°46′ N, 001°20′ W, UK National Grid SP 461 081). The climate is typical for southern England (mean air temperature 10.1 °C, precipitation 730 mm y^{-1} [31]). Wytham was selected for this project because it has been surveyed with ALS twice since 2007 (during both leaf-on and leaf-off conditions). Although situated on a hill, forest topography is mostly less than 10° and being a protected site the topography has not been altered during the period between or since the ALS surveys (Figure 1).

Both leaf-on and leaf-off LiDAR datasets were collected by the Natural Environment Research Council (NERC) Airborne Research Facility (ARF). Airborne LiDAR surveys were flown on 24 June 2014 and 9 March 2009 respectively. The leaf-on dataset flight parameters were ~2500 m agl (altitude) and ~134 knots (ground speed). The LiDAR instrument was a small-footprint Leica ALS50-II LiDAR system with full waveform and discrete recording capabilities (up to 4 returns per emitted pulse). The LiDAR pulse repetition frequency (PFR) was 96.8 kHz, field of view (FOV) was 35°, with 99.8% return rate and average point density of 0.918 m^2. For the leaf-off dataset, the flight parameters were ~1181 m agl at ~135 knots. The ALS instrument PFR measurements were at 84.4 KHz, with a 24° FOV, with 100% return rate. Mean return densities for the leaf-on and leaf-off datasets were 3.17 and 5.06 returns m^{-2} respectively, above the threshold density of 0.6 points m^{-2} where DTM generation is said to become inaccurate [32]. Furthermore, the density of the leaf-on dataset was approximately 62% of the leaf-off density, which is above the 50% threshold whereby DTM accuracies become statistically different, meaning they are comparable without normalisation [33,34].

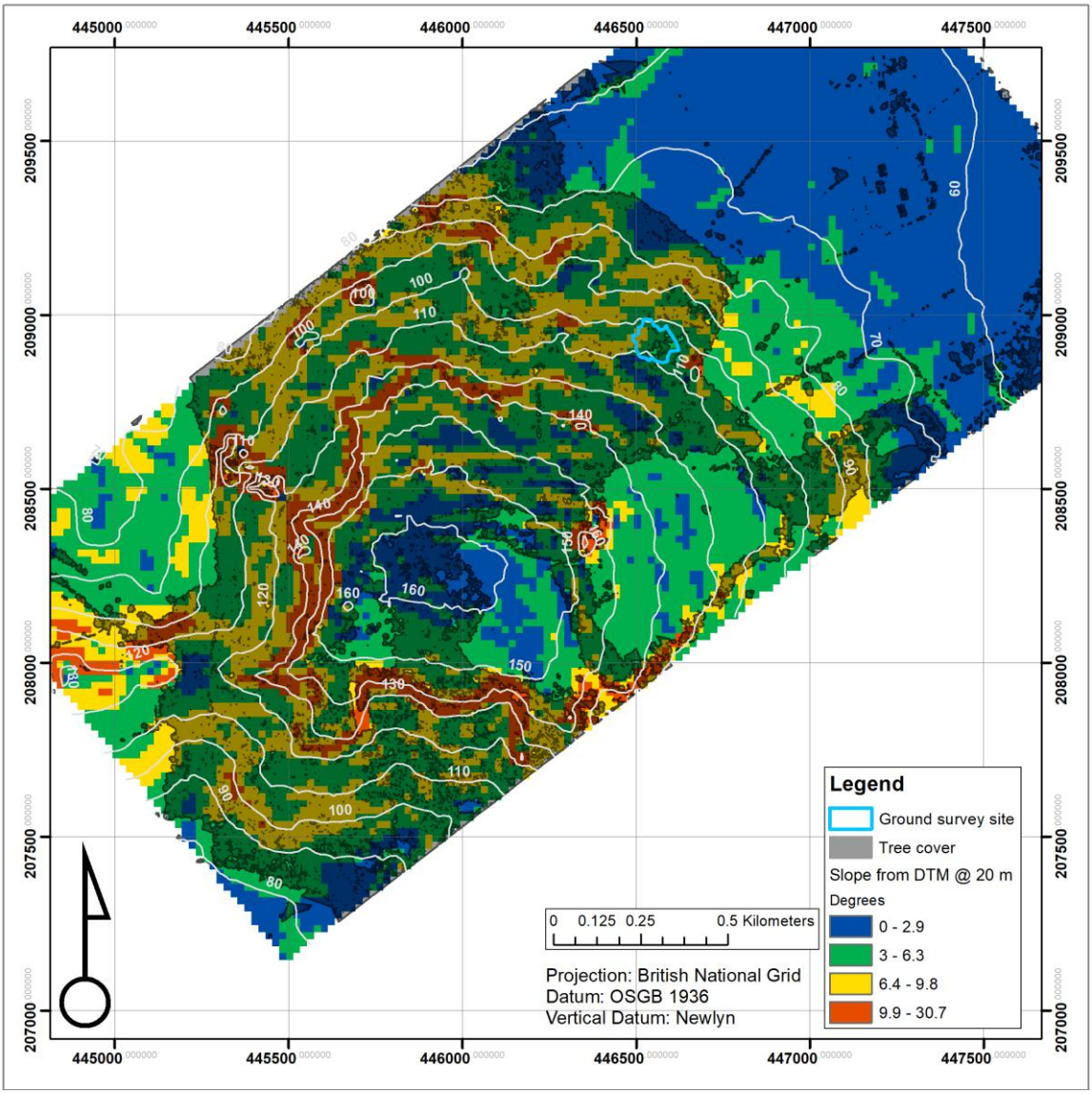

Figure 1. Slopes in Wytham woods (at 20 m resolution) with tree cover overlaid in dark grey. Both contours and slopes are derived from a ground-classified Airborne Laser Scanning (ALS) point cloud, filtered using elevation minima at 20 m resolution.

A site was selected based on its highly heterogeneous vegetation structure (Figure 2), including forest clearances as well as areas of dense canopy and understory vegetation, and its relatively flat topography. It was also situated centrally in the LiDAR swath, so that biases due to scan angle were equally distributed throughout the site [9]. Ground data for the reference DTM were collected at the selected site between 23–28 January 2017 using a Leica VIVA GS10 Global Navigation Satellite System with a baseline between the GNSS base station and survey site of approximately 950 m; the rover antenna was mounted on a 2 m survey pole. A Trimble M3 total station was used to measure ground points on and between the marked GNSS ground control points (GCPs). The instrument position was measured in all three locations using the GNSS antenna. The prism operator paced approximately 5 m between measurements, giving a final point density of approximately 596 points per hectare.

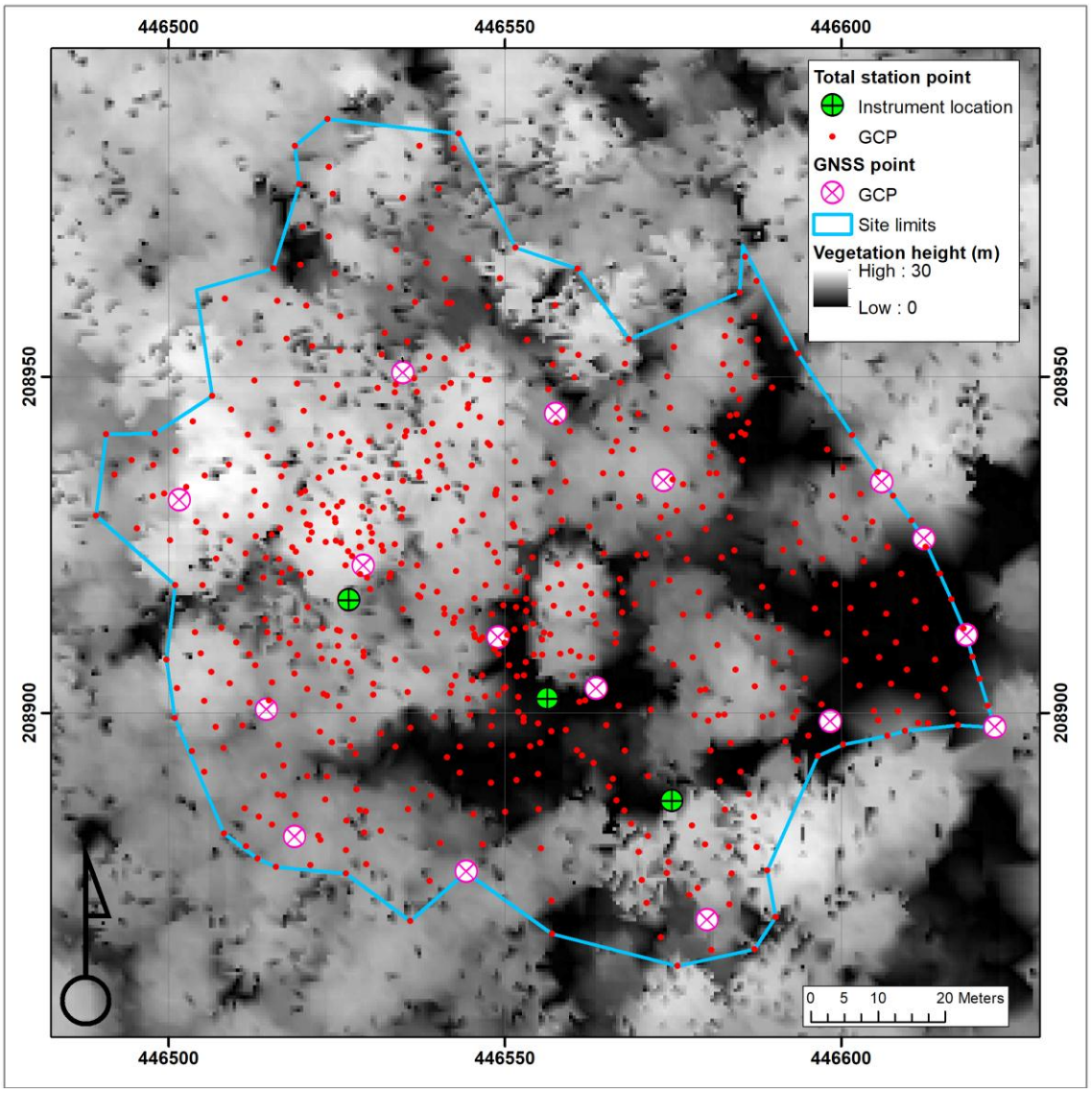

Figure 2. Survey area layout. Ground surveys conducted with Global Navigation Satellite Systems (GNSS) and total stations (TS) equipment overlapped. The three total station surveys were georeferenced using 16 of the most accurate GNSS points. An approximate site boundary is drawn around the outermost points.

Total station datasets provide very high accuracy point measurements in the X, Y, Z axes relative to the total station instrument. To georeference these positions to absolute coordinates (British National Grid OSGB36, Newlyn vertical datum), 16 matching GNSS-derived datapoints were used. The GNSS rover points were differentially corrected to the GNSS base station position in Leica Geo Office, which improves relative accuracy to within 0.04 m. Rinex files from a permanent Ordnance Survey base station (baseline from GNSS base station was 6.7 km) were used to improve absolute accuracy of both GNSS base station and rover points. Absolute accuracy in X, Y, Z axes of GNSS rover points ranged between 0.002 m and 0.034 m. Total station surveys were individually transformed from relative to absolute grid coordinates (OSGB36, OSTN02) using a least squares method using GNSS points (delta Easting/Northing/Elevation, X/Y/Z rotation (Table 2).

Table 2. Transformation statistics of TS datasets to GNSS control points (n = 16).

TS to GNSS	σX	σY	σZ	σXYZ
Mean (m)	0.000	0.000	0.000	0.023
Max (m)	0.037	0.058	0.048	0.001
RMSE (m)	0.016	0.030	0.022	0.023

To ensure the ALS dataset was georeferenced correctly, an additional four control sites were surveyed (Figure 3). The control sites were situated either on forest service roads (compacted gravel) or local roads (asphalt). A total of 438 TS control points were taken, using 21 GNSS control points distributed across four locations for transformation to absolute coordinates. The TS control points were rasterised (0.5 m resolution) in CloudCompare (v2.6.2) and were compared to ALS returns in the same area to calculate the transformation parameters. The same transformation was applied to the entire leaf-on ALS dataset (Table 3). At the 438 control points, vertical bias improved from −0.64 (1σ = 0.10 m) to 0.07 (1σ = 0.07 m), and overall accuracy improved from RMSE = 0.64 m to RMSE = 0.11 m. The ALS leaf-off dataset was aligned at the control locations to the reference dataset improving bias from −0.19 m to 0.002 m (±1σ = 0.22 mm).

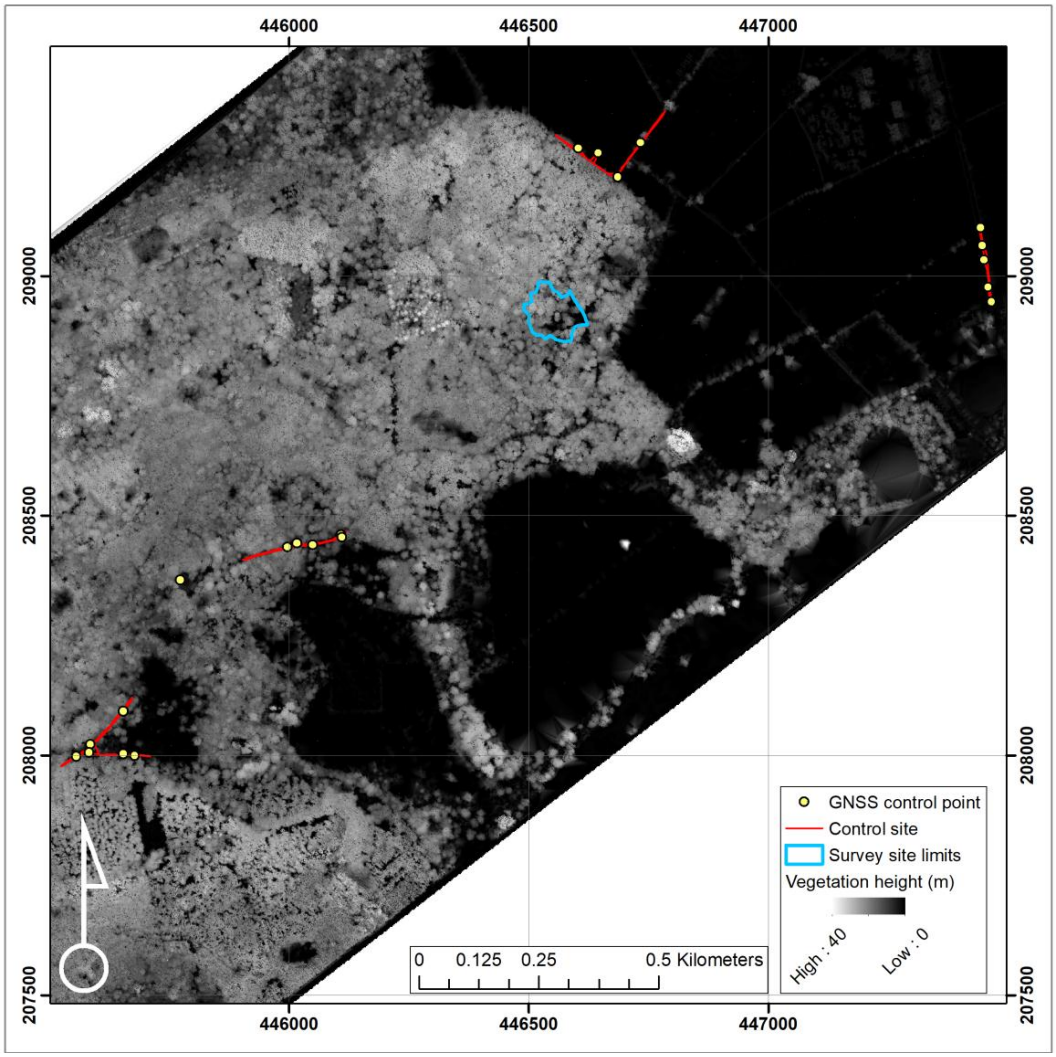

Figure 3. Control site locations, with GNSS control points visible as yellow dots, and the forest survey site outlined in blue.

Table 3. Transformation matrix of ALS point cloud based on 438 TS control points on uncovered, hard road surfaces.

Rotation	X	Y	Z	Translation
X	1	0.000012	0.000147	−0.06666
Y	-1×10^{-5}	1	−0.0001	0.021064
Z	−0.0001	0.000103	1	0.700736
	0	0	0	1

The ALS point clouds were classified as ground or non-ground using LAStools [35], by removing noise, and using the "lasground" tool which only considers last returns, and is based on a mesh simplification approach as outlined by [36]. DTMs were produced from ground returns using an Inverse Distance Weighting algorithm at 1 m resolution to account for site microtopography. This algorithm has proven to yield highly accurate DTMs [17]. A control dataset was produced from the TS ground control dataset (DTM_{TS}) using the same method (n = 657). The control DTM was subtracted from the ALS-derived DTM (DTM_{ALS}) to produce difference rasters. The height differences were taken at 1750 randomly located points (at least 1m apart to avoid repetition) within the survey grids (Figure 4).

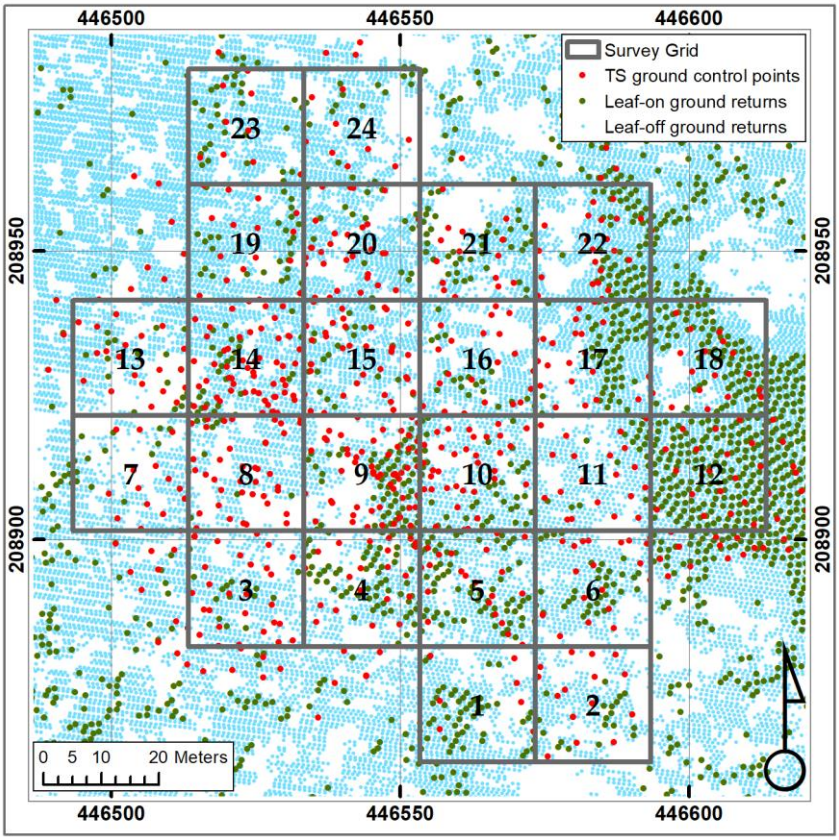

Figure 4. Ground point layout within the survey grid cells. All total station (TS) ground control points were used to a construct a digital terrain model (DTM), which was then used to assess the accuracy of the airborne laser scanning (ALS) derived DTMs, derived during leaf-on and leaf-off conditions. The numbered grid cells were used to extract vertical vegetation characteristics.

In order to explain the effects of vegetation on DTM accuracy, vertical vegetation structure was assessed using gap probability (Pgap) in the ALS leaf-on dataset. Pgap can be used to describe the amount of backscatter of large-footprint waveform LiDAR from vegetation surfaces, and has also been

applied to discrete return data at a plot level [1,19]. 20 m grid cells were used to optimise coverage of ALS and TS ground points (Figure 4), and the vertical vegetation structure was assessed for each cell. Using discreet return ALS data, three vertical vegetation strata were identified by examining the density of returns through the vegetation column in all 24 grid cells (Figure 5), and cross referencing this plot with observations made in the field. The three strata comprise of dense ground-cover plants such as bramble (*Rubus fruticosus*), nettles (*Urtica dioica*), and brackens (e.g., *Pteridium aquilinum*) which peak at 3.5 m (red line), mid-story vegetation up to 10 m which include large shrubs and short-stature trees such as alder (*Alnus glutinosa*), field maple (*Acer campestre*) and hazel (*Corylus avellane*) (as well as immature Oak, Ash and Sycamore trees), and above 10 m are dominant canopy Oak (*Quercus robur*), Ash (*Fraxinus excelsior*) and Sycamore (*Acer pseudoplatanus*).

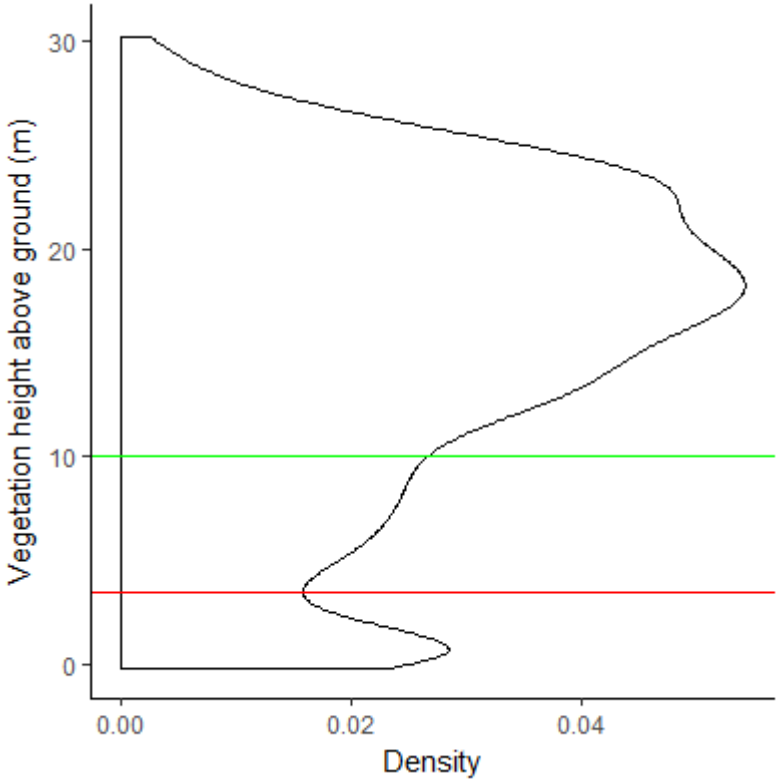

Figure 5. Density plot of discreet ALS returns in the vertical vegetation column across the whole site. The red line shows the vertical upper limit of the ground-cover stratum, and the green line shows the upper limit of the mid-canopy stratum.

For each 20 m grid cell, the vertical gap probability (Pgap, metric describing the proportion of vegetation returns at specific heights) was calculated for each stratum (adapted from [1]).

$$Pgap(z) = 1 - \frac{\sum w_i\,(z_i)}{W}$$

where W is the per grid cell sum of the number of returns, w is the sum of ground returns per grid cell within the vertical limits of each stratum, z.

The grid cells were categorised according to the relative differences between Pgap in all three strata using two cluster analysis techniques, *K*-means and hierarchical clustering (via rattle, hclust and cluster packages) in RStudio (v1.0.136). The optimal value of parameter K (number of clusters based on minimisation of within-cluster sum of squares) was estimated using "the elbow method" by plotting the variance explained as a function of the number of clusters [37]). Once the optimal number of clusters was calculated (K = 6 in this case), the grid cells were categorized into clusters using a

K-means fit algorithm, and were analysed and validated by representing the result of the *K*-means fit graphically in a 3D plot (Figure 6). This was compared to a cluster dendogram (Figure 7) in which categories are produced using hierarchical clustering employing a Euclidean distance matrix as an input for the clustering algorithm to reduce the intra-cluster variance. Using the vertical profile density plots (Figure 7), ground observations (Figure 8), and the grid cell distribution in relation to the canopy (Figure 9), the six categories (A to F) were defined and are described in Table 4.

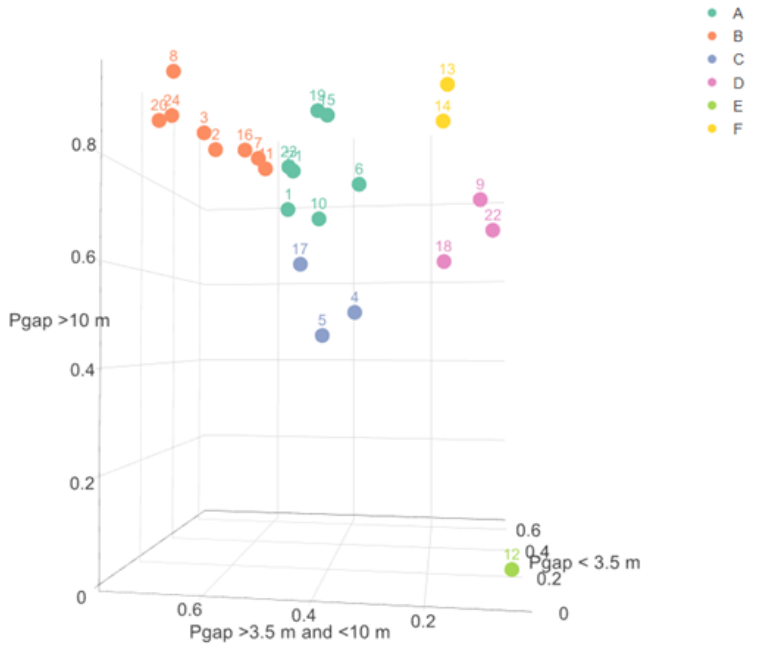

Figure 6. Numbered forest grid cells from Figure 4 classified into six distinct structural categories (colours), based on the Pgap values for three distinct vertical strata (<3.5 m, >3.5 and <10 m, >10 m) and a hierarchical clustering method (Figure 7).

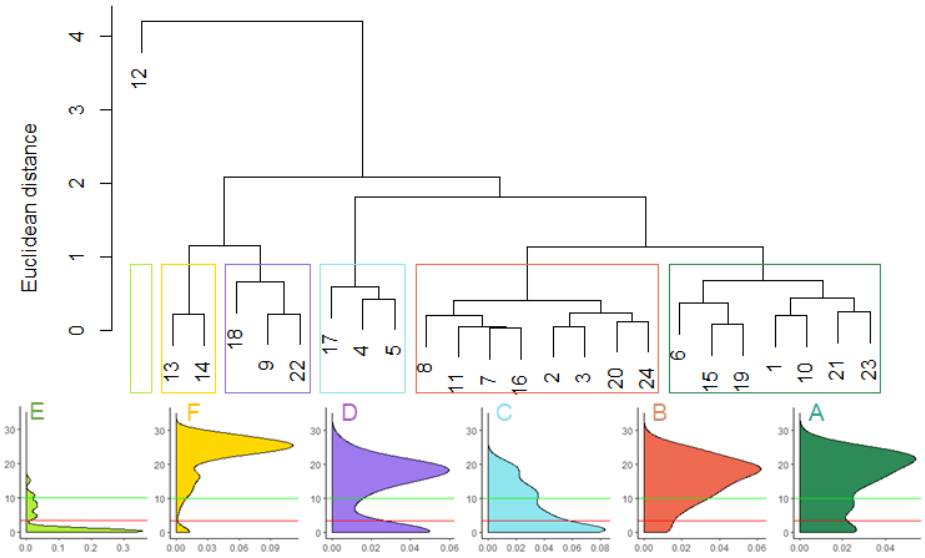

Figure 7. Dendogram showing the inter- and intra-cluster relationships in vertical vegetation structure between grid cells. For clarity, each final category is assigned a colour and letter (cf Figure 6). Below each cluster are the vertical profile density plots, showing the density of ALS returns as a function of height above ground (m) for each category.

Figure 8. Some examples of vertical vegetation structural categories in leaf-off conditions; (**a**) dense undergrowth (brambles and dead ferns) with mid-story small trees, and few large trees, characteristic of structural category C; (**b**) structural category A has dense understory amongst mid-story vegetation and tall canopy trees; (**c**) tall canopy trees dominate category F, and (**d**) shows the clearing edge and clearing groups (C and D). Photos taken January 2017 by Jake Simpson.

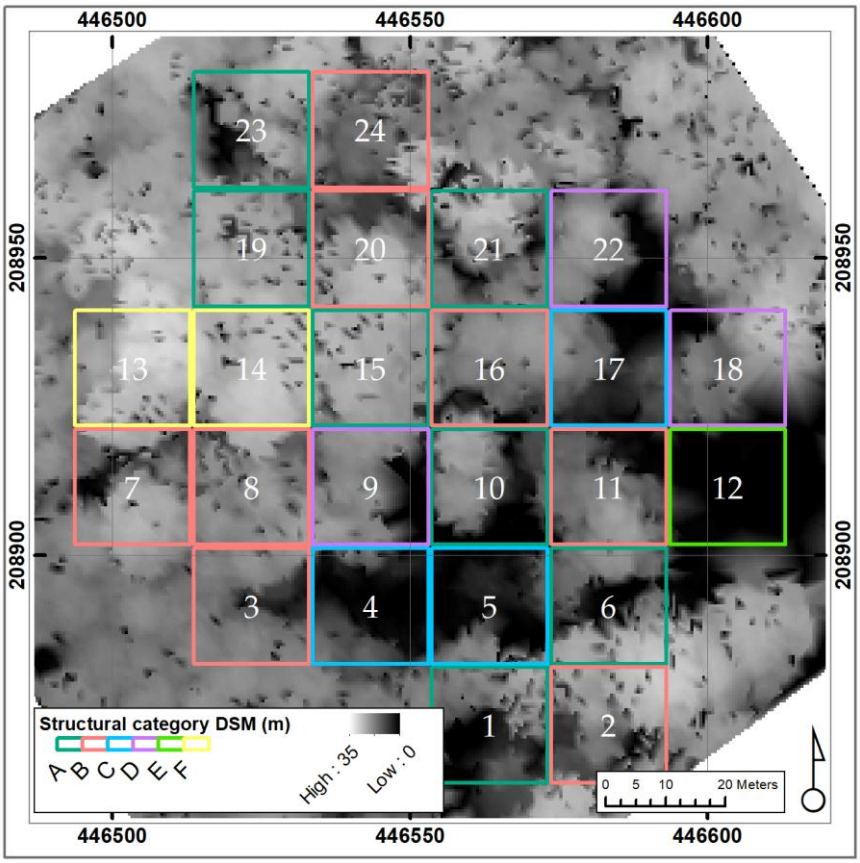

Figure 9. Grid cell vegetation structure categories (see Figure 7 and Table 4) shown superimposed on a vegetation height model (digital surface model/DSM).

Table 4. Descriptions of each vertical vegetation structure category, with the mean Pgap of grid cells within each category, and 1 standard deviation of the mean.

Structural Category	Description	Location	Mean Pgap	1σ
A	Some undergrowth and mid-story, very dense canopy	Partially-closed canopy forest	0.87	0.03
B	Little undergrowth, dense mid-story and very dense canopy	Partially-closed canopy forest	0.93	0.01
C	Very dense undergrowth, dense mid-story, sparse/no canopy	Clearing edge	0.73	0.01
D	Dense undergrowth, sparse mid-story and dense canopy	Clearing edge, small forest gap	0.72	0.07
E	Some undergrowth, sparse/no mid-story and canopy	Clearing	0.17	NA
F	Sparse/no undergrowth and mid-story, very dense canopy	Closed canopy forest	0.92	0.03

Accuracy assessments were performed by differencing the TS-derived DTM and ALS-derived DTMs at 1m resolution (DTM_{TS} and DTM_{ALS} respectively). Firstly, the effects of site microtopography (slope) on DTM accuracy were examined using a Generalized Additive Model (GAM) (which is useful for uncovering patterns in continuous data with non-normal distributions). Then, the effects of vertical vegetation structure on DTM accuracy were examined in three ways, (1) by comparing DTM accuracy in leaf on and leaf off conditions (because only some understory vegetation is evergreen in this plot), (2) by comparing the different vertical vegetation structures (Pgap categories) in both leaf-on and leaf-off datasets, (3) comparing mean DTM accuracy per grid cell as a function of Pgap values for each vertical stratum. To assess the statistical significance of differences in DTM accuracy between the different conditions and vegetation categories, the data were assessed for heteroscedasticity and unequal variances using Bartlett and Levene tests respectively. All data were heteroscedastic; therefore comparisons were made using White-adjusted Anova from the car package in R, and pairwise comparisons are made using Tukey's honest significant difference tests.

3. Results

The median slope within the plot was 5.7°. The relationship between vertical DTM residuals and slope at 1m resolution was examined using a non-parametric GAM. Slope has no meaningful effect on residuals, with slope explaining 0.25% of the deviance, and a poor goodness of fit (adjusted $R^2 = 0.002$, Figure 10).

Leaf-off conditions improved overall DTM accuracy by 61 cm ($RMSE_{leaf\text{-}off}$ = 0.22 m vs. $RMSE_{leaf\text{-}on}$ = 0.83 m, n = 1750) at 1 m resolution (Figure 11), demonstrating that leaf-on vegetation induces larger positive DTM errors. Leaf-on and leaf-off DTM residuals were significantly different (F = 3086, df = 1, $p < 0.001$) and consequently, RMSE differences between leaf-on and leaf-off DTM were also significantly different (F = 20.02, df = 1, $p < 0.01$).

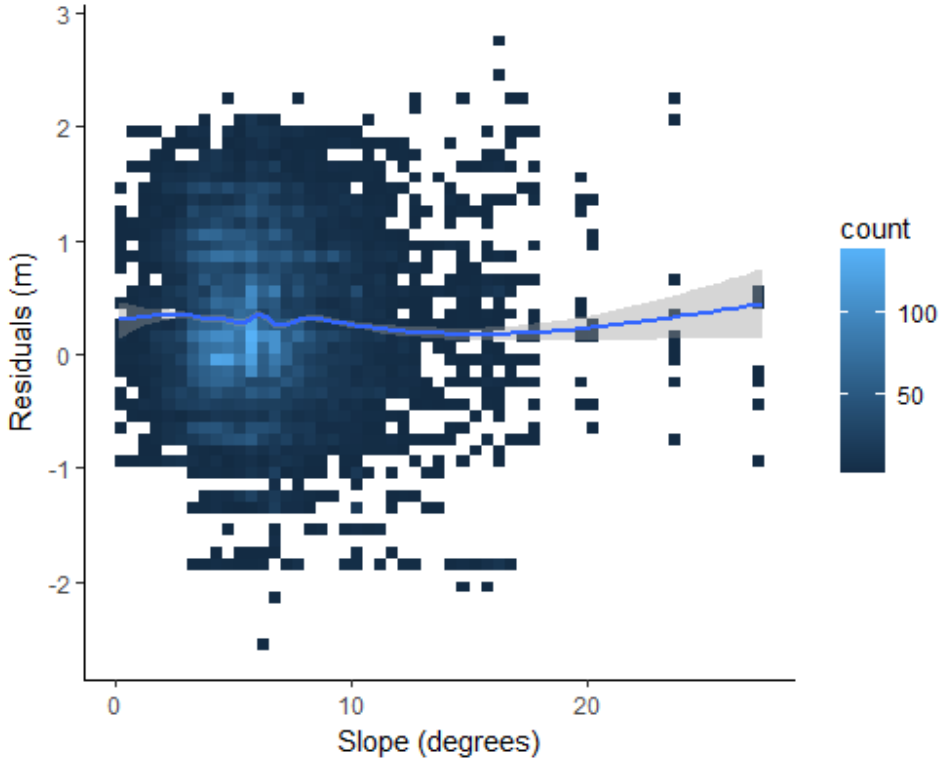

Figure 10. A 2-dimensional distribution showing the effects of slope on DTM accuracy with the Generalized Additive Model (GAM) fit shown as a blue line (with 95% confidence interval in grey). There is no discernible relationship between slope and accuracy at 1 m DTM resolution (n = 1750).

In each of the six vertical vegetation structure categories of Table 4, DTM accuracy (RMSE) was better in leaf-off than leaf-on conditions (Figure 12), with the largest/smallest difference being 0.81/0.10 m in structural category C/E (edge of clearing, very dense undergrowth, with some mid-story and no canopy/grassy clearing). Category C and D grid cells show inaccurate DTM heights in both leaf-on and leaf-off conditions, apparently because of the persistence of dense undergrowth vegetation (such as brambles) over the winter. Thick canopy layers are more penetrable by LiDAR than is dense undergrowth, as seen by the better accuracies in categories A–B vs. those in C–D. The range of vertical residual errors is represented in Figure 13. There were only 14 pairs which were not significantly different from each other. In leaf-off conditions, residuals in all structural categories were not significantly different to another and were close to zero (mean = 0.07 m, 1s.d. = 0.20 m). In leaf-on conditions (with the exception of category E), there was marked differences between structural categories, which were considerable higher than in leaf-off conditions (mean = 0.71 m, 1s.d. = 0.43 m).

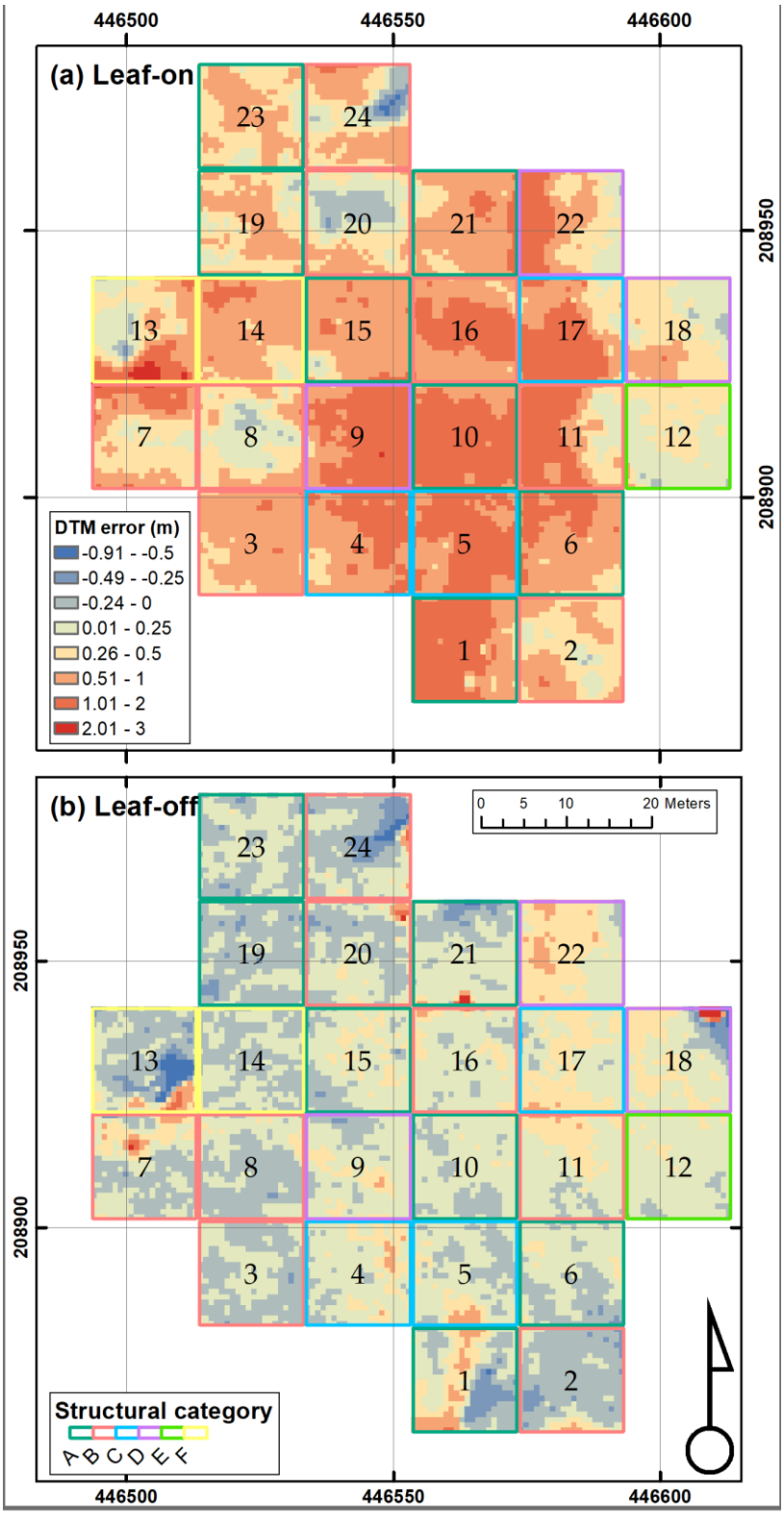

Figure 11. Digital Terrain Model (DTM) error (DTM_{TS}-DTM_{ALS}) in both leaf-on (**a**) and leaf-off (**b**) conditions at 1 m resolution, and shown in relation to the six vegetation structural categories of Table 4. DTM error is clearly higher across the site during leaf-on conditions, but in both DTMs the highest accuracy is in grid cell 12 (vegetation structure category E, forest clearing). The dark red patches in (**a**) spanning grid cells 1, 4, 5, 6, 9, 10, 11, 16, and 17 coincide with large areas of bramble, fern and nettle undergrowth.

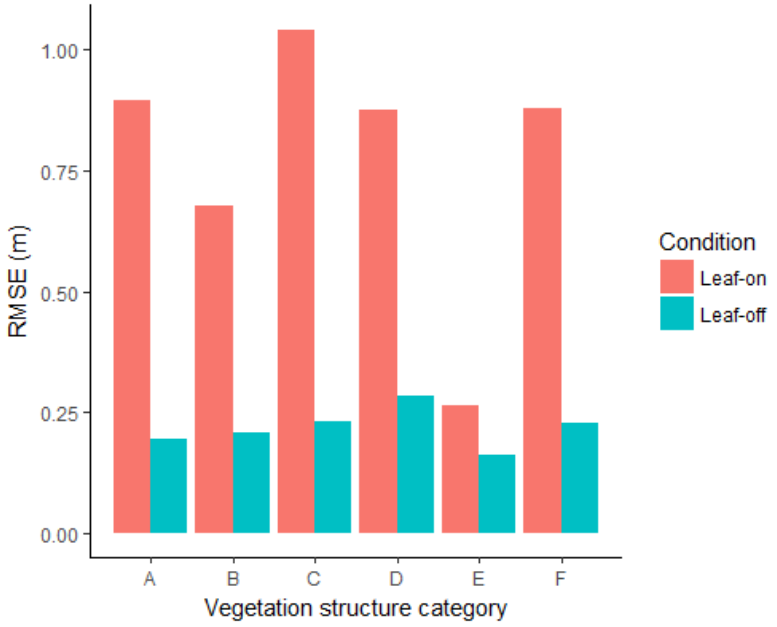

Figure 12. Digital Terrain Model (DTM) accuracy in the six different vegetation categories of Table 4, in both leaf-on and leaf-off conditions.

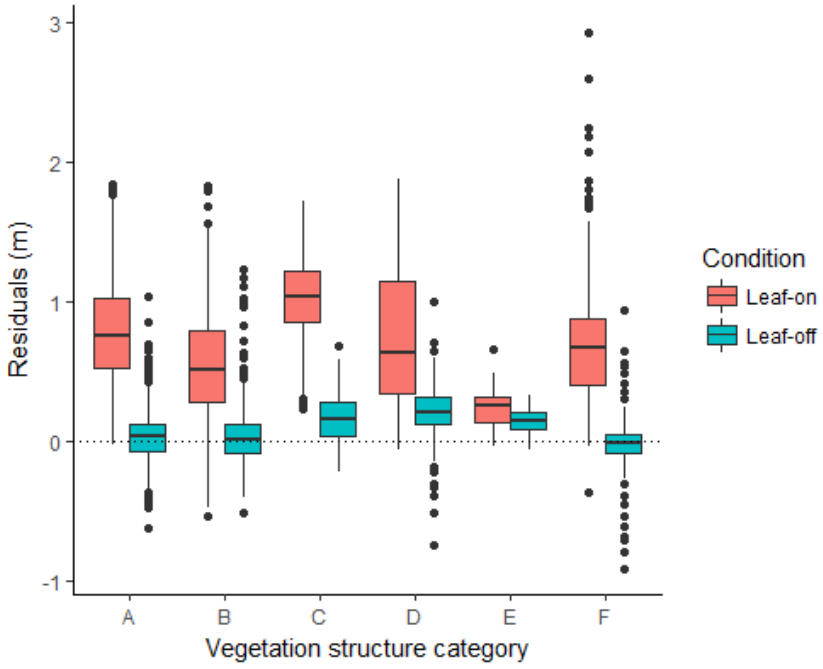

Figure 13. Boxplot of Digital Terrain Model (DTM) residuals between vegetation structural categories in both leaf-on and leaf-off conditions (n = 1750). These errors were measured at randomly distributed points, and are the differences between the DTM_{TS} (1m resolution) and DTM_{ALS} (1 m resolution). Central horizontal lines, boxes, whiskers and dots indicate the median, middle 50%, outer 50% of data points, and outliers respectively. Errors in leaf-on conditions are consistently higher than leaf-off conditions for each vertical vegetation structure category.

The relative impact of vegetation density (Pgap) at each vertical stratum on DTM error was assessed at the grid cell-scale for the leaf-on DTM (because the greatest errors are found in leaf-on conditions). DTM error increases with vegetation density at the lowest stratum only (<3.5 m).

Vegetation density at the mid- and upper strata (3.5–10 m, and >10 m respectively) has little effect on DTM error (Figure 14).

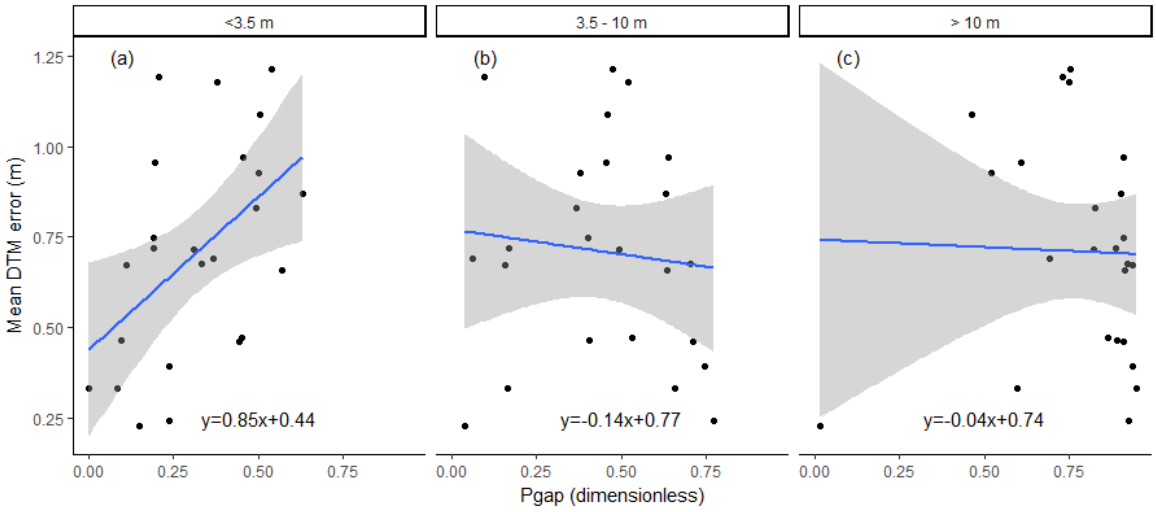

Figure 14. DTM error is mainly caused by increasing density of vegetation below 3.5 m tall, as shown in (**a**). DTM error is relatively independent of vegetation density above 3.5 m (**b**,**c**). The relationships are all weak (r^2 = 0.24, r^2 = 0.01, r^2 = 0.001 in (**a**–**c**) respectively), The blue lines and grey shaded areas denote the linear trend-line and 95% confidence interval respectively. Linear equations are marked in each plot.

4. Discussion

To date, few studies using airborne laser scanning (ALS)-derived Digital Terrain Models (DTMs) in forests have included the type of adequate ground control required to assess DTM accuracy, and fewer have quantitatively assessed how vegetation vertical structure affects this accuracy in broadleaf forests. While many forest applications of ALS survey data may tolerate accuracies of better than 0.5 m (such as forest height and above-ground biomass applications), applications such as tropical and temperate peatland depth of burn (DoB) mapping and peat subsidence estimation are far more sensitive to these errors because changes in ground height needing to be identified are typically less than 0.5 m in magnitude [17,20,23]. The results of the present study suggest that without an adequate ground control scheme, such applications may be prone to significant positive biases, especially in areas of leaf-on, open canopy forest with large amounts of ground cover.

Our assessment of the effects of vertical vegetation structure in a heterogenous forest plot on DTM accuracy has performed accuracy assessments between ALS-derived DTMs and a reference DTM derived from ground surveys using a total station and GNSS. Results demonstrate that leaf-on vegetation causes greater DTM error (RMSE = 0.83 m) than leaf-off vegetation (RMSE = 0.22) across all vegetation categories. Furthermore, DTM accuracy is not affected by all vegetation structures equally; with dense understory vegetation such as ferns and brambles causing the greatest positive DTM errors. Grassland vegetation yields the most accurate DTMs. This is consistent with previous qualitative [20] and quantitative assessments in forest environments [11]. [15] measured DTM accuracy as a function of canopy density in a Malaysian woodland, however they did not attempt to use vertical vegetation structure as an explanatory variable. Here we have shown that ALS datasets themselves can be used to extract information about vegetation structure that relates directly to the DTM accuracy, showing that low-stature ground cover plants (<3.5 m) obscure most ground returns and cause greater error (RMSE > 1 m).

The results of this study are demonstrably applicable to other settings, and complement other studies; e.g., ref. [17] found dense ground-covering vegetation obscured more ground returns than

intact tropical peat swamp forest, and overall leaf-on DTM errors were similar to those in [11] (also in temperate broadleaf forest). Limitations remain, including (1) A relatively low return density (approximately 3–5 returns m^{-2}), because [38] found DTM errors in tropical broadleaf forests increased with decreasing ALS return density, suggesting that DTM errors could be reduced by increasing return density (e.g., reducing flight altitude). (2) Errors induced by leaf litter were not quantified; DTM_{TS} was produced using exact ground points from a total station survey, however DTM_{ALS} will always be erroneous in the presence of leaf litter because measurements cannot penetrate the leaf litter. Here the best accuracies in leaf-off conditions were approximately 20 cm, with mean residuals of less than 0.04 m (1sd < 0.18 m) for structural categories with little vegetation <3.5 m tall (structural categories A, B and F, e.g., grid cells 1, 2, 11, 13), which could be caused by the leaf-litter layer. (3) The results presented here show how DTM accuracy is relatively affected by vegetation structure, and as such they cannot be applied absolutely to other forest environments (i.e., these are not correction factors).

Using detailed surveys made in just under 1 ha of deciduous forest, this study has demonstrated how different vertical vegetation structures affect DTM accuracy. Although the overall study area is relatively small, the sample features a variety of different vertical structures which are found across the woodland (i.e., a mosaic of clearings, dense undergrowth, mid-story trees, and mature canopy trees on low-relief slope) which is likely to represent the wider forest environment. The different ratios of vegetation strata are represented by the vegetation vertical categories and are sampled at least once within the plot (with the exception of category E, grassland clearing). The size of sampling area is also consistent with previous studies [8,13].

Further work could include a continuation of the analysis presented in Figure 14, whereby DTM error is directly compared to vegetation structure metrics (e.g., Pgap). If this relationship could be directly modelled using data from more reference plots, and evaluated over a larger area, DTM error might be predictable from vegetation structure alone.

5. Conclusions

This study highlights the requirement for ground controls for DTM extraction from ALS point clouds in forest areas, especially in areas where undergrowth or ground cover vegetation is prevalent. For studies which require high DTM accuracy (e.g., tropical peat swamp forest depth of burn measurement), it is recommended that extensive ground control points are used across a range of vegetation structures to assess the accuracy of DTMs [20], in order to account for biases caused by vegetation cover. Precautions for the greatest DTM errors should be taken in areas characterized by dense ground-cover vegetation, since ground returns are most likely to be obscured here. These areas could easily be identified using Pgap statistics or even a simple canopy height model. Future studies should aim to quantify these DTM biases, as in environments involving burning of organic soils, they may lead to very large over-estimates in greenhouse gas emissions calculations.

Acknowledgments: This project is part of, and funded by, a Natural Environment Research Council (NERC) CASE studentship awarded to Jake E. Simpson and contributes to the outputs of NERC grants NE/L009811/1 and NE/N01555X. An equipment grant was awarded for the use of the GNSS by NERC Geophysical Equipment Facility, to whom we are very grateful for their support. Both leaf-on and leaf-off datasets were supplied by NERC. We thank the Conservator of Wytham Woods, Nigel Fisher and Yadvinder Malhi, University of Oxford for their permission to conduct the field work. Further thanks are extended to Phil Wilkes (UCL) for his assistance in the field and guidance afterwards, and Alex Kemp (UCL) and Krzystof Bluszcz for helping with the surveys.

Author Contributions: Jake E. Simpson conceived and designed the experiments; Jake E. Simpson and Thomas E. L. Smith performed the experiments; Jake E. Simpson analyzed the data; Jake E. Simpson, Thomas E. L. Smith and Martin J. Wooster contributed analysis tools; Jake E. Simpson wrote the paper.

Conflicts of Interest: The authors declare no conflict of interest. The founding sponsors had no role in the design of the study; in the collection, analyses, or interpretation of data; in the writing of the manuscript, and in the decision to publish the results.

References

1. Wilkes, P.; Jones, S.D.; Suarez, L.; Haywood, A.; Mellor, A.; Woodgate, W.; Soto-Berelov, M.; Skidmore, A.K. Using discrete-return airborne laser scanning to quantify number of canopy strata across diverse forest types. *Methods Ecol. Evol.* **2016**, *7*, 700–712. [CrossRef]
2. Koch, B.; Heyder, U.; Weinacker, H. Detection of individual tree crowns in airborne LIDAR data. *Photogramm. Eng. Remote Sens.* **2006**, *72*. [CrossRef]
3. Rahman, M.Z.A.; Gorte, B. Individual Tree Detection Based on Densities of High Points of High Resolution Airborne LIDAR. Available online: http://www.isprs.org/proceedings/xxxviii/4-c1/sessions/Session12/6790_Rahman_Proc.pdf (accessed on 26 October 2017).
4. Clark, M.L.; Clark, D.B.; Roberts, D.A. Small-footprint lidar estimation of sub-canopy elevation and tree height in a tropical rain forest landscape. *Remote Sens. Environ.* **2004**, *91*, 68–89. [CrossRef]
5. Estornell, J.; Ruiz, L.A.; Velázquez-Martí, B.; Hermosilla, T. Analysis of the factors affecting LiDAR DTM accuracy in a steep shrub area. *Int. J. Digit. Earth* **2011**, *4*, 521–538. [CrossRef]
6. Bao, Y.; Cao, C.; Zhang, H.; Chen, E.; He, Q.; Huang, H.; Li, Z.; Li, X.; Gong, P. Synchronous estimation of DTM and fractional vegetation cover in forested area from airborne LIDAR height and intensity data. *Sci. China Ser. E* **2008**, *51*, 176–187. [CrossRef]
7. Hyyppä, H.; Yu, X.; Hyyppä, J.; Kaartinen, H.; Kaasalainen, S.; Honkavaara, E.; Rönnholm, P. Factors affecting the quality of DTM generation in forested areas. *Int. Arch. Photogramm. Remote Sens. Spat. Inf. Sci.* **2005**, *36*, 85–90.
8. Reutebuch, S.E.; McGaughey, R.J.; Andersen, H.-E.; Carson, W.W. Accuracy of a high-resolution lidar terrain model under a conifer forest canopy. *Can. J. Remote Sens.* **2003**, *29*, 527–535. [CrossRef]
9. Su, J.; Bork, E. Influence of vegetation, slope, and lidar sampling angle on DEM accuracy. *Photogramm. Eng. Remote Sens.* **2006**, *72*, 1265–1274. [CrossRef]
10. Tinkham, W.T.; Smith, A.M.S.; Hoffman, C.; Hudak, A.T.; Falkowski, M.J.; Swanson, M.E.; Gessler, P.E. Investigating the influence of LiDAR ground surface errors on the utility of derived forest inventories. *Can. J. For. Res.* **2012**, *42*, 413–422. [CrossRef]
11. Hodgson, M.E.; Jensen, J.R.; Schmidt, L.; Schill, S.; Davis, B. An evaluation of LIDAR- and IFSAR-derived digital elevation models in leaf-on conditions with USGS Level 1 and Level 2 DEMs. *Remote Sens. Environ.* **2003**, *84*, 295–308. [CrossRef]
12. Wasser, L.; Day, R.; Chasmer, L.; Taylor, A. Influence of Vegetation Structure on Lidar-derived Canopy Height and Fractional Cover in Forested Riparian Buffers During Leaf-Off and Leaf-On Conditions. *PLoS ONE* **2013**, *8*, e54776. [CrossRef] [PubMed]
13. Hansen, E.H.; Gobakken, T.; Næsset, E. Effects of Pulse Density on Digital Terrain Models and Canopy Metrics Using Airborne Laser Scanning in a Tropical Rainforest. *Remote Sens.* **2015**, *7*, 8453–8468. [CrossRef]
14. Jubanski, J.; Ballhorn, U.; Kronseder, K.; Franke, J.; Siegert, F. Detection of large above-ground biomass variability in lowland forest ecosystems by airborne LiDAR. *Biogeosciences* **2013**, *10*, 3917–3930. [CrossRef]
15. Salleh, M.R.M.; Ismail, Z.; Rahman, M.Z.A. Accuracy assessment of lidar-derived digital terrain model (dtm) with different slope and canopy cover in tropical forest region. *Ann. Photogramm. Remote Sens. Spat. Inf. Sci.* **2015**, *II-2/W2*, 183–189. [CrossRef]
16. Englhart, S.; Franke, J.; Keuck, V.; Siegert, F. Aboveground biomass estimation of tropical peat swamp forests using SAR and optical data. In Proceedings of the 2012 IEEE International Geoscience and Remote Sensing Symposium (IGARSS), Munich, Germany, 22–27 July 2012; pp. 6577–6580.
17. Konecny, K.; Ballhorn, U.; Navratil, P.; Jubanski, J.; Page, S.E.; Tansey, K.; Hooijer, A.; Vernimmen, R.; Siegert, F. Variable carbon losses from recurrent fires in drained tropical peatlands. *Glob. Chang. Biol.* **2016**, *22*, 1469–1480. [CrossRef] [PubMed]
18. Ren, H.C.; Yan, Q.; Liu, Z.J.; Zuo, Z.Q.; Xu, Q.Q.; Li, F.F.; Song, C. Study on analysis from sources of error for Airborne LIDAR. *IOP Conf. Ser. Earth Environ. Sci.* **2016**, *46*, 12030. [CrossRef]
19. Lovell, J.L.; Jupp, D.L.B.; Culvenor, D.S.; Coops, N.C. Using airborne and ground-based ranging lidar to measure canopy structure in Australian forests. *Can. J. Remote Sens.* **2003**, *29*, 607–622. [CrossRef]
20. Ballhorn, U.; Siegert, F.; Mason, M.; Limin, S. Derivation of burn scar depths and estimation of carbon emissions with LiDAR in Indonesian peatlands. *Proc. Natl. Acad. Sci. USA* **2009**, *106*, 21213–21218. [CrossRef] [PubMed]

21. Fowler, A.; Kadatskiy, V. Accuracy and error assessment of terrestrial, mobile and airborne LIDAR. In Proceedings of the American Society of Photogrammetry and Remote Sensing Conference (ASPRP 2011), Milwaukee, WI, SUA, 1–5 May 2011.
22. Razak, K.A.; Santangelo, M.; Van Westen, C.J.; Straatsma, M.W.; de Jong, S.M. Generating an optimal DTM from airborne laser scanning data for landslide mapping in a tropical forest environment. *Geomorphology* **2013**, *190*, 112–125. [CrossRef]
23. Reddy, A.D.; Hawbaker, T.J.; Wurster, F.; Zhu, Z.; Ward, S.; Newcomb, D.; Murray, R. Quantifying soil carbon loss and uncertainty from a peatland wildfire using multi-temporal LiDAR. *Remote Sens. Environ.* **2015**, *170*, 306–316. [CrossRef]
24. Wang, Y. Trends in atmospheric haze induced by peat fires in Sumatra Island, Indonesia and El Niño phenomenon from 1973 to 2003. *Geophys. Res. Lett.* **2004**, *31*. [CrossRef]
25. Davenport, I.J.; Bradbury, R.B.; Anderson, G.Q.A.; Hayman, G.R.F.; Krebs, J.R.; Mason, D.C.; Wilson, J.D.; Veck, N.J. Improving bird population models using airborne remote sensing. *Int. J. Remote Sens.* **2000**, *21*, 2705–2717. [CrossRef]
26. Onaindia, M.; Dominguez, I.; Albizu, I.; Garbisu, C.; Amezaga, I. Vegetation diversity and vertical structure as indicators of forest disturbance. *For. Ecol. Manag.* **2004**, *195*, 341–354. [CrossRef]
27. Næsset, E.; Gjevestad, J.G. Performance of GPS precise point positioning under conifer forest canopies. *Photogramm. Eng. Remote Sens.* **2008**, *74*, 661–668. [CrossRef]
28. Simpson, J.E.; Wooster, M.J.; Smith, T.E.L.; Trivedi, M.; Vernimmen, R.R.E.; Dedi, R.; Shakti, M.; Dinata, Y. Tropical Peatland Burn Depth and Combustion Heterogeneity Assessed Using UAV Photogrammetry and Airborne LiDAR. *Remote Sens.* **2016**, *8*, 1000. [CrossRef]
29. Jaskierniak, D.; Lane, P.N.J.; Robinson, A.; Lucieer, A. Extracting LiDAR indices to characterise multilayered forest structure using mixture distribution functions. *Remote Sens. Environ.* **2011**, *115*, 573–585. [CrossRef]
30. Wilkes, P.; Jones, S.D.; Suarez, L.; Haywood, A.; Woodgate, W.; Soto-Berelov, M.; Mellor, A.; Skidmore, A.K. Understanding the Effects of ALS Pulse Density for Metric Retrieval across Diverse Forest Types. *Photogramm. Eng. Remote Sens.* **2015**, *81*, 625–635. [CrossRef]
31. Simpson, J.E.; Slade, E.; Riutta, T.; Taylor, M.E. Factors Affecting Soil Fauna Feeding Activity in a Fragmented Lowland Temperate Deciduous Woodland. *PLoS ONE* **2012**, *7*, e29616. [CrossRef] [PubMed]
32. Jia, Y.; Lan, T.; Peng, T.; Wu, H.; Li, C.; Ni, G. Effects of point density on DEM accuracy of airborne LiDAR. In Proceedings of the 2013 IEEE International Geoscience and Remote Sensing Symposium—IGARSS, Melbourne, VIC, Australia, 21–26 July 2013; pp. 493–496.
33. Bater, C.W.; Wulder, M.A.; Coops, N.C.; Nelson, R.F.; Hilker, T.; Nasset, E. Stability of Sample-Based Scanning-LiDAR-Derived Vegetation Metrics for Forest Monitoring. *IEEE Trans. Geosci. Remote Sens.* **2011**, *49*, 2385–2392. [CrossRef]
34. Liu, X.; Zhang, Z.; Peterson, J.; Chandra, S. The effect of LiDAR data density on DEM accuracy. In Proceedings of the International Congress on Modelling and Simulation (MODSIM07), Christchurch, New Zealand, 10–13 December 2007; pp. 1363–1369.
35. Isenburg, M. LAStools—Efficient Tools for LiDAR Processing. Available online: https://rapidlasso.com/ (accessed on 26 October 2017).
36. Axelsson, P. Processing of laser scanner data—algorithms and applications. *ISPRS J. Photogramm. Remote Sens.* **1999**, *54*, 138–147. [CrossRef]
37. Kodinariya, T.M.; Makwana, P.R. Review on determining number of Cluster in K-Means Clustering. *Int. J. Adv. Res. Comput. Sci. Manag. Stud.* **2013**, *1*, 90–95.
38. Leitold, V.; Keller, M.; Morton, D.C.; Cook, B.D.; Shimabukuro, Y.E. Airborne LIDAR-based estimates of tropical forest structure in complex terrain: Opportunities and trade-offs for REDD+. *Carbon Balance Manag.* **2015**, *10*. [CrossRef] [PubMed]